Paper Folding: Modeling and Simulation

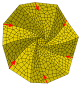

Sören Bartels

University of Freiburg, Germany

SFB S^3 Kickoff Meeting, Aachen, September 22, 2022

Numerical analysis for nonlinear and multiscale problems

Joint work with Andrea Bonito (Texas A&M), Peter Hornung (TU Dresden), Philipp Tscherner (U Freiburg)

Title pictures: NASA Starshade simulation [Bonito, Guignard & Morvant '2x]

Nature & Art: Unfolding of a ladybird's wings, curved origami

Source: University of Tokyo,
The Sydney Morning Herald

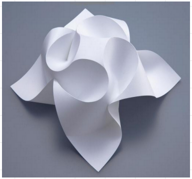

Source: Jun Mitani,
Curved-Folding Origami Design

Biomimetics: Shading structure inspired by underwater carnivorous plant

Aldrovanda vesiculosa
Source: Axel Körner

Flectofold construction
Source: Axel Körner

Isometries: Piecewise smooth isometry $y : \omega \to \mathbb{R}^3$

$$(\nabla y)^{\mathsf{T}} \nabla y = \mathbb{I}_{2\times 2}$$

Folding arcs: Folding curve $b : I \to \overline{\omega}$ maintains geodesic curvature κ under isometric deformation

Darboux frames: Normals n^ℓ define Darboux frames

$$r^\ell = [\gamma', n^\ell, \gamma' \times n^\ell] \in SO(3), \quad \gamma = y \circ b$$

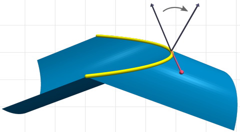

Folding angle: Since frames share tangent γ'

$$r^2 = R(\theta, \gamma') r^1$$

Curvatures: *Geodesic* $\kappa = (r_1^\ell)' \cdot r_2^\ell$ and *normal* $\mu^\ell = (r_1^\ell)' \cdot r_3^\ell$ curvatures and *torsion* $\tau^\ell = (r_2^\ell)' \cdot r_3^\ell$ related via, unless $\theta \in 2\pi\mathbb{Z}$,

$$\kappa \sin\left(\frac{\theta}{2}\right) = \pm \mu^\ell \cos\left(\frac{\theta}{2}\right), \quad \tau^2 = \tau^1 + \theta'$$

Related: Simpler version in [Duncan & Duncan '82]

Implications: For deformed plate along crease C

- if $\kappa = 0$ then either unfolded or folded back or θ constant and $\mu^\ell = 0$
- if $\kappa \neq 0$ then either unfolded or $\mu^\ell \neq 0$ and θ uniquely defined

Related: Periodic kirigami structures (e.g., maps and deployable structures)

- [Liu, Choi, Mahadevan '21] 17 patterns define periodic tilings of the plane
- [James & Liu '22+] Origami structures with curved tiles between creases

3D hyperelasticity: Energy functional for deformation $y : \Omega \to \mathbb{R}^3$

$$I^{3d}[y] = \int_\Omega W(x, \nabla y)\,\mathrm{d}x - \int_\Omega f \cdot y\,\mathrm{d}x$$

with isotropic and objective density $W : \mathbb{R}^{3\times 3} \to \mathbb{R}_{\geq 0}$

$$W(\mathbb{I}_{3\times 3}) = 0, \quad W(QFR) = W(F) \quad \forall Q, R \in SO(3)$$

Prepared material: Material softer along arc $C \subset \overline{\omega}$

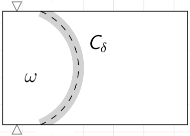

Model reduction: $\Omega = \omega \times (-\delta/2, \delta/2)$

- narrow region C_δ, soft material $\mathbb{C}_\delta$
- ∇y discontinuous along C

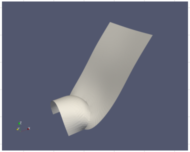

For isometry $y \in H^2(\omega \setminus C; \mathbb{R}^3) \cap W^{1,\infty}(\omega; \mathbb{R}^3)$

$$I_{\mathrm{fold}}[y] = \frac{1}{2}\int_{\omega\setminus C} |D^2 y|^2\,\mathrm{d}x - \int_\omega f \cdot y\,\mathrm{d}x$$

Proof: [B., Bonito & Hornung '22] following [Friesecke, James & Müller '02]

Discretization aspects:

- fourth order problem with pointwise nonlinear constraint
- approximation of curved interface with gradient discontinuity

Conceptual dG approach: Discrete energy functional

$$I_h[y_h] = \frac{1}{2}\int_\omega |D_h^2 y_h|^2 \,\mathrm{d}x - \int_\omega f y_h \,\mathrm{d}x + \frac{\gamma_0}{2}\int_{\mathcal{E}} h_{\mathcal{E}}^{-\alpha} |[\![y_h]\!]|^2 \,\mathrm{d}s + \frac{\gamma_1}{2}\int_{\mathcal{E}\setminus C_h} h_{\mathcal{E}}^{-\beta} |[\![\nabla_h y_h]\!]|^2 \,\mathrm{d}s$$

with constraint

$$(\nabla_h y_h)^{\mathsf{T}} \nabla_h y_h = \mathbb{I}_{2\times 2} \quad \forall x_q \in \mathcal{Q}_h$$

Analytical difficulties: Parameter selection and interface accuracy

- optimal consistency avoiding overpenalization
- approximation order for approximated interface
- choice of quadrature points to avoid locking

Related: dG for 2nd order interface problems [Cangiani, Georgoulis & Sabawi '18]

Linear model: Small deflections, no isometry condition

$$I_{\mathrm{lin}}[u] = \frac{1}{2}\int_{\omega\setminus C} |D^2 u|^2 \,\mathrm{d}x - \int_\omega f u \,\mathrm{d}x, \quad u \in H^1(\omega) \cap H^2(\omega \setminus C)$$

Euler-Lagrange equation: Biharmonic problem away from C

$$\Delta^2 u = f \quad \text{in } \omega \setminus C$$

Interface conditions: Along interface C

$$[\![u]\!] = 0, \quad \partial_n \nabla u = 0, \quad [\![\partial_n \Delta u]\!] = 0$$

DG method: For curved partition $\mathcal{T}_h$ with interface C_h $(= C)$

$$\begin{aligned}(f, v_h) = (D^2 u, D_h^2 v_h)_{L^2(\omega\setminus C_h)} &+ \langle \{\!\{\partial_n \nabla u\}\!\}, [\![\nabla_h v_h]\!]\rangle_{L^2(\mathcal{E}\setminus C_h)} + \langle \{\!\{\partial_n \nabla_h v_h\}\!\}, [\![\nabla u]\!]\rangle_{L^2(\mathcal{E}\setminus C_h)} \\ &- \langle \{\!\{\partial_n \Delta u\}\!\}, [\![v_h]\!]\rangle_{L^2(\mathcal{E})} - \langle \{\!\{\partial_n \Delta_h v_h\}\!\}, [\![u]\!]\rangle_{L^2(\mathcal{E})} \\ &+ \gamma_1 \langle h^{-1}[\![\nabla u]\!], [\![\nabla_h v_h]\!]\rangle_{L^2(\mathcal{E}\setminus C_h)} + \gamma_0 \langle h^{-3}[\![u]\!], [\![v_h]\!]\rangle_{L^2(\mathcal{E})}\end{aligned}$$

Lax-Milgram: For appropriate BCs and γ_0, γ_1 sufficiently large

$$\exists!\, u_h \in V_h \quad a_h(u_h, v_h) = (f, v_h) \quad \forall v_h \in V_h$$

Curved elements: Isoparametric $\psi_T : \widehat{T} \to T$ with [Lenoir '86, Ern & Guermond '21]

$$\|D^s \psi_T\|_{L^\infty(\widehat{T})} \le c h_T^s, \quad 2 \le s \le k+1$$

- Interpolation estimates from [Bonito, Nochetto & Ntogkas '21]

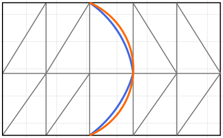

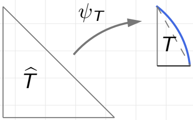

Discretization: For $C = C_h$ standard procedure gives

$$\|u - u_h\|_{dG} \le \begin{cases} h^{k-1} \|u\|_{H^{k+1}(\omega \setminus C)} & \text{for } k > 2 \\ h \, \|u\|_{H^4(\omega \setminus C)} & \text{for } k = 2 \end{cases}$$

Interface approximation: For $u \in H^2(\omega \setminus C)$ and $u_k \in H^2(\omega \setminus C_h)$

$$\|D_h^2(u - \widetilde{u}_k)\| \le c h^{k-1} \big(\|D_h^2 \widetilde{u}_k\| + \|\nabla \widetilde{u}_k\| \big)$$

Idea of proof: Map u_k from $\Omega \setminus C_h$ to $\Omega \setminus C$ via $\widetilde{u}_k|_T = u_k \circ \Phi_T$

Test 1: Two sides clamped, no vs. quadratic interface

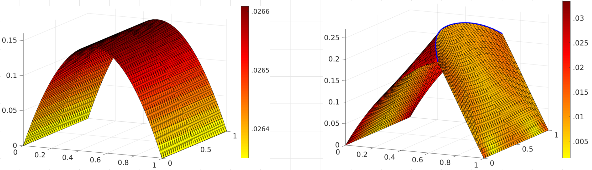

Test 2: One side clamped, one boundary point fixed, no vs. quadratic interface

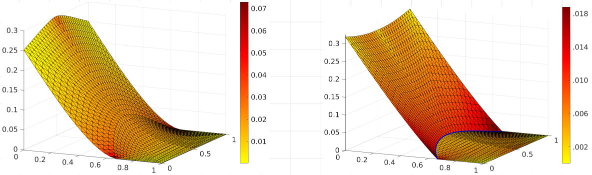

Conclusion: Crease significantly affects bending behavior

Test 1: Linear interface approximation, quadratic elements

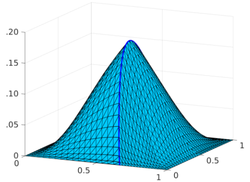

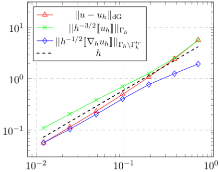

Test 2: Quadratic interface approximation, quadratic elements

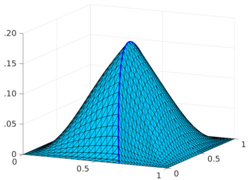

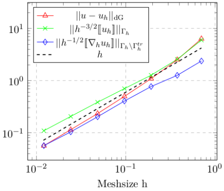

Observation: No difference for quadratic vs. linear crease approximation

Discrete Hessian: From [Ern & DiPietro '10, Pryer '14, Bonito, Nochetto & Ntogka '20]

$$H_h[y_h] = D_h^2 y_h + \sum_{e\in\mathcal{E}} b_e([\![y_h]\!]) - \sum_{e\in\mathcal{E}\setminus C_h} r_e([\![\nabla_h y_h]\!])$$

with local lifting operators

$$\int_{\omega_e} b_e(\psi) : \tau_h \,\mathrm{d}x = \int_e \{\mathrm{div}_h \tau_h\} \cdot n_e \psi \,\mathrm{d}s, \quad \int_{\omega_e} r_e(\phi) : \tau_h \,\mathrm{d}x = \int_e \{\tau_h\} n_e \cdot \phi \,\mathrm{d}s$$

Consistency: For test function ϕ with $\mathrm{supp}\,\phi$ not intersecting C

$$\int_\omega H_h(y_h) : \phi \,\mathrm{d}x = \int_\omega y_h \cdot \mathrm{div}\,\mathrm{Div}\,\phi \,\mathrm{d}x - \int_{\mathcal{E}} [\![y_h]\!]\, \mathrm{Div}[\phi - \mathcal{I}_h\phi] \cdot n_{\mathcal{E}} \,\mathrm{d}s$$

$$+ \int_{\mathcal{E}} [\![\nabla_h y_h]\!][\phi - \mathcal{I}_h \phi] n_{\mathcal{E}} \,\mathrm{d}s + \int_\omega \big(B_{\mathcal{E}}([\![y_h]\!]) - R_{\mathcal{E}}([\![\nabla_h y_h]\!])\big) : [\phi - \mathcal{I}_h\phi] \,\mathrm{d}x,$$

with sum of green terms vanishing by definitions of b_e and r_e

For $h \to 0$ and $H_h(y_h)$ bounded in L^2 and w.r.t. $\|\cdot\|_{dg}$

$$\int_\omega \psi : \phi \,\mathrm{d}x = \lim_{h\to 0} \int_\omega H_h(y_h) : \phi \,\mathrm{d}x = \int_\omega y \cdot \mathrm{div}\,\mathrm{Div}\,\phi \,\mathrm{d}x$$

Discrete energy: With discrete Hessian

$$I_h[y_h] = \frac{1}{2}\int_\omega |H_h(y_h)|^2 \,\mathrm{d}x - \int_\omega f y_h \,\mathrm{d}x$$
$$+ \frac{\gamma_1}{2}\|h^{-1/2}[\![\nabla_h y_h]\!]\|^2_{L^2(\mathcal{E}\setminus C_h)} + \frac{\gamma_0}{2}\|h^{-3/2}[\![y_h]\!]\|^2_{L^2(\mathcal{E})}$$

Relaxed isometry: For suitable tolerance and quadrature points

$$\left|\nabla y_h(x)^\mathsf{T}\nabla y_h(x) - \mathbb{I}_{2\times 2}\right| \le \varepsilon_h \quad \forall x \in \mathcal{Q}_h$$

Well-posedness: Unconditional existence of discrete minimizers from coercivity

$$\alpha_0 |y_h|^2_{dg} \le I_h[y_h]$$

for all $\gamma_0, \gamma_1 > 0$ (fixed) with

$$|y_h|^2_{dg} = \|D_h^2 y_h\|^2 + \|h^{-1/2}[\![\nabla_h y_h]\!]\|^2_{L^2(\cup\mathcal{E}\setminus C_h)} + \|h^{-3/2}[\![y_h]\!]\|^2_{L^2(\cup\mathcal{E})}$$

Stability: If $I_h[y_h] \le c$ then $\|y_h\|_{dg} \le c'$ and weak limits y satisfy

$$I[y] \le \liminf_{h\to 0} I_h[y_h]$$

Gradient descent: Compute tangential corrections $d_t y^n \in \mathcal{F}[y^{n-1}]$ via

$$\big(d_t y^n, w\big)_\star + \alpha\big(D^2 y^n, D^2 w\big) = 0$$

for all $w \in \mathcal{F}[y^{n-1}]$, with linearization of $[G]^2 = G^\mathsf{T} G$

$$\mathcal{F}[\widehat{y}] = \big\{ w \in W : \nabla w^\mathsf{T} \nabla \widehat{y} + \nabla \widehat{y}^\mathsf{T} \nabla w = 0 \big\},$$

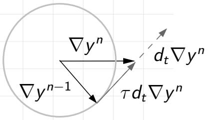

set $y^n = y^{n-1} + \tau d_t y^n$

Proposition [B. '13]. If $\big[\nabla y^0\big]^2 = \mathbb{I}_{2\times 2}$ and $\|\nabla w\| \le c_\star \|w\|_\star$

$$\text{(i)} \quad I[y^n] + \frac{\tau}{2}\|d_t y^n\|_\star^2 \le I[y^{n-1}],$$

$$\text{(ii)} \quad \|[\nabla y^n]^2 - \mathbb{I}_{2\times 2}\|_{L^1} \le c_\star^2 \tau I[y^0].$$

- *unconditional* stability and well-posedness, choose $w = d_t y^n$
- no projection – progressive violation of isometry constraint

$$[\nabla y^n]^2 = [\nabla y^{n-1}]^2 + \tau^2 [d_t \nabla y^n]^2 = \cdots = \mathbb{I}_{2\times 2} + \tau^2 \sum_{\ell=1}^{n} [d_t \nabla y^\ell]^2$$

Test 1: Curved arc on rectangular plate with compressive BCs

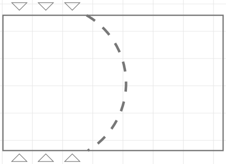

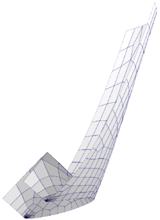

Test 2: Ring with central folding curve compressed at two opposite points

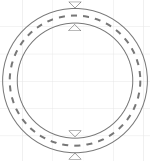

Challenges: Choice of initial deformations, instabilities, lack of regularity

Methodology: Lack of Euler–Lagrange equations, use Γ-convergence

- *Stability*, i.e., if $I_h[y_h]$ is bounded then there exists $y \in H^2_{\rm iso}(\omega \setminus C)$
$$y_h \rightharpoonup y \quad \text{and} \quad I[y] \le \liminf_{h\to 0} I_h[y_h]$$
- *Consistency*, i.e., for all $y \in H^2_{\rm iso}(\omega \setminus C)$ exists $(y_h)_{h>0}$
$$y_h \rightharpoonup y \quad \text{and} \quad I[y] = \lim_{h\to 0} I_h[y_h]$$

Theorem [De Giorgi '75] Convergence of (almost) minimizers

Approximability: Density of smooth folded (nearly) isometries as [Hornung '08] for unfolded isometries or [Bonito et al. '21] approximate isometries

Smooth minimizers: If $y \in H^3(\omega \setminus C)$ then $y_h = \mathcal{I}_h y_h$ satisfy
$$D_h^2 y_h \to D^2 y \quad \text{strongly in } L^2(\omega \setminus C) \quad \Longrightarrow \quad I_h[y_h] \to I[y]$$

Optimality: Density result determines choice of parameters

Babuška's plate paradox: Solutions on polygonal domains of linear bending problem not convergent to solution on curved domain for simple support (free normal on boundary)

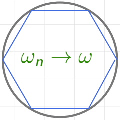

$$-\Delta^2 u_n = 1$$
$$u_n|_{\partial\omega_n} = 0$$

$u_n \not\to u$

Clamped BC: No failure for $u|_{\partial\omega} = \nabla u|_{\partial\omega} = 0$ (density of $C_0^\infty(\omega)$)

Critical identity: Variational interpretation [Bonito '22+]

$$\int_\omega |D^2 u|^2 \,\mathrm{d}x = \int_\omega |\Delta u|^2 \,\mathrm{d}x + \int_{\partial\omega} \kappa |\nabla u|^2 \,\mathrm{d}x$$

with curvature $\kappa = 0$ for piecewise linear boundary

Isometries: Developable surfaces characterized by $|D^2 y|^2 = |\Delta y|^2 = H^2$

Questions: Babuška's paradox in view of isometries

- Consequence of incorrect linearization ?
- Interpretation of interface condition for folds ?

Observation: Cardboard box shows material fatigue

Explanation: No finite energy path among isometries

Föppl-von Kármán model (no fold): Different scaling of in-plane deformation and deflection [Friesecke, James & Müller '06]

$$I_{\mathrm{fvk}}[u,w] = \frac{\gamma^2}{2}\int_\omega |D^2 w|^2 \,\mathrm{d}x + \frac{1}{2}\int_\omega |\varepsilon(u) + \nabla w \otimes \nabla w|^2 \,\mathrm{d}x - \int_\omega f w \,\mathrm{d}x$$

Experiment: Quasistationary switching via f between spherical states for compressive BCs

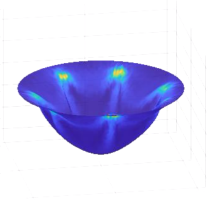

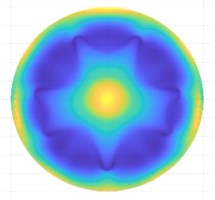

External Link

Analysis: Break of symmetry [Conti, Olbermann & Tobasco '15]

Question: Relation to thin sheet folding of insect wings?

[Haas & Wootton '96] Hindwing folding of cockroach *Diploptera punctata*

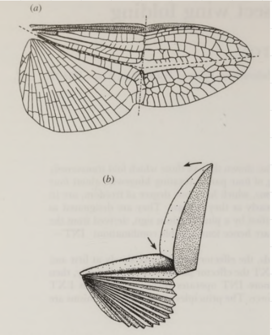

Source: [Haas & Wootton '96]

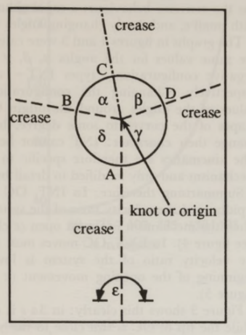

Source: [Haas & Wootton '96]

Interpretation: Discrete curvature realization of flapping mechanism

- Large deformation folding from 3D hyperelasticity
- Characterization of admissible folds
- DG method suitable for 4th order curved interface problem

- Ongoing and future work:
  - Density result for folded isometries
  - Fast iterative solution, initial configurations
  - Nonlinear variant of Babuška's plate paradox ?

- A source of inspiration:

Summary

- Large deformation folding from 3D hyperelasticity
- Characterization of admissible folds
- DG method suitable for 4th order curved interface problem

- Ongoing and future work:
  - Density result for folded isometries
  - Fast iterative solution, initial configurations
  - Nonlinear variant of Babuška's plate paradox ?

- A source of inspiration:

i'm lovin' it®

- Large deformation folding from 3D hyperelasticity
- Characterization of admissible folds
- DG method suitable for 4th order curved interface problem

- Ongoing and future work:
  - Density result for folded isometries
  - Fast iterative solution, initial configurations
  - Nonlinear variant of Babuška's plate paradox ?

- A source of inspiration:

Mathematics

i'm lovin' it®